THE ANATOLIAN JOURNAL OF CARDIOLOGY

Official journal of the TURKISH SOCIETY OF CARDIOLOGY

Circulating Quiescin Sulfhydryl Oxidase and Risk of Cardiovascular Disease: A Mendelian Randomization and Post-GWAS Analysis

ABSTRACT

Background: To systematically evaluate the causal associations between circulating quiescin sulfhydryl oxidase (QSOX) family enzymes and cardiovascular diseases (CVDs) using Mendelian randomization (MR) and post-Genome-Wide Association Study (post-GWAS) analyses.

Methods: The authors integrated protein quantitative trait locus (pQTL) data for plasma QSOX from the INTERVAL and deCODE studies with CVD GWAS summary statistics from large-scale biobank datasets and disease-specific consortia. Discovery MR analyses were followed by meta-analysis and independent replication. Post-GWAS annotation using the FUMA platform was performed to delineate the pQTL architecture of circulating QSOX2 and to prioritize likely causal variants. Summary-data-based Mendelian randomization (SMR) was applied to confirm direct effects of QSOX2 on CVDs and to characterize its regulatory networks at individual *cis* and *trans* pQTLs.

Results: Initial *pan*-MR analyses suggested risk-increasing associations of circulating QSOX2 with several CVDs, but showed substantial SNP-level heterogeneity. Regional and functional annotation identified pleiotropic signals originating from *distal* and *trans* regions, and prioritized the missense variant *rs12380852* as the leading causal candidate, predicted to impair QSOX2 structural stability and enzymatic activity. Notably, *cis*-MR and SMR analyses restricted to the QSOX2 locus revealed consistent protective effects against atrial fibrillation (AF) and heart failure (HF). Summary-data–based Mendelian randomization on *trans* pQTL *rs3184504* (a *SH2B3* missense variant) linked SH2B3-mediated inflammatory pathways to QSOX2 *trans* regulation.

Conclusion: The authors' findings suggest a protective role of circulating QSOX2 in AF and HF. The prioritized causal variants and identified *trans*-regulatory pathways may serve as targets for future functional validation and druggable design.

Keywords: Cardiovascular disease, Mendelian randomization, quiescin sulfhydryl oxidase, pQTL, post-GWAS

INTRODUCTION

Cardiovascular disease (CVD) remains the leading cause of morbidity and mortality worldwide, underscoring the urgent need for novel biomarkers and therapeutic targets.[1] Circulating proteins have emerged as attractive candidates owing to their accessibility in plasma and their potential to reflect or directly mediate disease processes. Disulfide bonds are critical for numerous cardiovascular proteins, from extracellular matrix (ECM) components that provide structural scaffolding to signaling molecules such as B-type natriuretic peptide (BNP), whose bioactivity depends on a specific disulfide-bonded conformation.[2-4] Enzymes that regulate disulfide bond formation and repair, such as the thioredoxin system and protein disulfide isomerase, have been extensively implicated in cardiovascular thrombotic disease and vascular remodeling.[5-7] Distinct from these systems, the quiescin sulfhydryl oxidase (QSOX) family, comprising QSOX1 and QSOX2, catalyzes the de novo formation of disulfide bonds with the concurrent reduction of oxygen to hydrogen peroxide in the Golgi apparatus and the extracellular space.[8,9] Increasing evidence has linked QSOX enzymes to cardiovascular phenotypes,

Copyright@Author(s) - Available online at anatoljcardiol.com.
Content of this journal is licensed under a Creative Commons Attribution-NonCommercial 4.0 International License.

ORIGINAL INVESTIGATION

Xinyu Che[1,2#]
Ao Chen[2-6#]
Yan Xia[2-6#]
Zheng Yang[2]
Xia Shao[7]
Binbin Yu[2]
Danbo Lu[2-6,8]
Jiaqi Ma[2-6]
Zhangwei Chen[2-6]
Juying Qian[1-6,8,9]
Junbo Ge[2-6]

[1]*Shanghai Institute of Infectious Disease and Biosecurity, Fudan University, Shanghai, China*
[2]*Department of Cardiology, Shanghai Institute of Cardiovascular Diseases, Zhongshan Hospital, Fudan University, China*
[3]*National Clinical Research Center for Interventional Medicine, Shanghai, China*
[4]*State Key Laboratory of Cardiovascular Diseases, Zhongshan Hospital, Fudan University, China*
[5]*NHC Key Laboratory of Ischemic Heart Diseases, China*
[6]*Key Laboratory of Viral Heart Diseases, Chinese Academy of Medical Sciences, China*
[7]*Department of Hematology, Shanghai General Hospital, Shanghai Jiaotong University School of Medicine, Shanghai, China*
[8]*Department of Cardiology, Shanghai Geriatric Medical Center, Shanghai, China*
[9]*State Key Laboratory of Medical Neurobiology, MOE Frontier Center for Brain Science, Fudan University, Shanghai, China*

Corresponding author:
Juying Qian
✉ qian.juying@zs-hospital.sh.cn

Received: May 23, 2026
Accepted: August 31, 2026
Available Online Date: October 30, 2026

Cite this article as: Che X, Chen A, Xia Y, *et al*. Circulating quiescin sulfhydryl oxidase and risk of cardiovascular disease: a Mendelian randomization and post-GWAS analysis. *Anatol J Cardiol*. 2026;XX(X):X-X.

[#]These authors (Xinyu Che, Ao Chen, and Yan Xia) contributed equally to this work.

DOI: 10.14744/AnatolJCardiol.2026.5239

including heart failure (HF), hypertension (HTN), and atrial fibrillation (AF).[10-12] However, whether these associations are causal remains unclear.

Mendelian randomization (MR) provides a powerful framework for inferring causal effects of exposures on outcomes by leveraging genetic variants as instrumental variables (IVs). When integrated with protein quantitative trait loci (pQTL) data, MR enables systematic evaluation of circulating proteins as causal contributors to disease risk.[13] Ideally, *cis*-acting variants are preferred in pQTL-based MR studies to capture direct protein effects, whereas *trans* pQTLs may inform regulatory networks involving gene products at the *trans* locus.[14] Early applications of MR on plasma proteins, however, were constrained by the limited availability of suitable genetic instruments. Recently, large-scale biobank studies with expanded sample sizes, broader proteome coverage, and deeper sequencing have substantially improved instrument quality.[15,16] When combined with post-Genome-Wide Association Study (post-GWAS) analyses, these data enable more effective dissection of the proteomic architecture of CVD and comprehensive molecular interpretation of disease-associated GWAS loci.[17] Notably, this genetic evidence-based approach has driven the clinical targeting of proprotein convertase subtilisin-kexin type 9 and angiopoietin-like 3 for lipid control and coronary heart disease (CHD) risk reduction.[18-20]

In this study, the authors aimed to systematically evaluate the causal roles of circulating QSOX family enzymes in CVDs from a genetic perspective. Using pQTL data from the INTERVAL and deCODE studies alongside large-scale GWAS outcome data, the authors first performed MR analyses to identify and validate potential causal associations. Next, the authors conducted post-GWAS annotation with the Functional Mapping and Annotation (FUMA) platform to delineate the pQTL architecture of circulating QSOX2 and to prioritize likely causal variants. Finally, the authors applied summary-data-based Mendelian randomization (SMR) to assess whether QSOX2 functions as a causal mediator in *cis*, linking identified genetic variants to disease, and to characterize its regulatory networks in *trans*.

HIGHLIGHTS

- Cis-Mendelian randomization (MR) analysis reveals protective effects of circulating QSOX2 against atrial fibrillation (AF) and heart failure (HF).
- Pan-MR risk-increasing signals are driven by pleiotropic distal and trans protein quantitative trait loci (pQTLs), explaining the observed heterogeneity.
- Summary-data-based Mendelian randomization analysis conducted on cis pQTL *rs12380852*, a missense variant associated with lower circulating QSOX2 levels and predicted to impair its function, supports QSOX2 as a causal mediator connecting *rs12380852* to AF and HF.
- Trans-SMR of *rs3184504* reflects a regulatory network involving QSOX2 that links SH2B3-mediated inflammatory pathways to cardiovascular conditions.

METHODS

Study Design and Data Sources

This study employed a 2-sample MR framework integrated with post-GWAS annotation. The analysis proceeded in 2 stages: discovery using INTERVAL pQTLs and FinnGen outcomes, followed by meta-analysis and independent validation. For discovery, plasma QSOX1 and QSOX2 pQTL data were obtained from the UK INTERVAL study, which measured protein levels in 3301 healthy participants using the SomaScan platform.[21] The CVD outcomes of interest were aortic aneurysm, atrial fibrillation, coronary heart disease, heart failure, hypertension, peripheral artery disease, stroke, ischemic stroke, intracerebral hemorrhage, transient ischemic attack, and venous thromboembolism (AA, AF, CHD, HF, HTN, PAD, STR, IS, ICH, TIA, and VTE). Disease GWAS summary statistics for the initial screen were obtained from the FinnGen consortium (data freeze May 5, 2021, available via OpenGWAS), comprising 218 792 individuals.[22,23] Significant MR results from the FinnGen screen were subsequently meta-analyzed with those from disease-specific consortia.[24-28] For replication, the authors used pQTL data from the Iceland deCODE study, which profiled 35 559 participants on the SomaScan platform, together with publicly available FinnGen–UK Biobank (UKB) meta-analysis GWAS data (https://public-metaresults-fg-ukbb.finngen.fi/).[15] These resources were used to validate the associations between circulating QSOX2 and CVDs (AF, HF, CHD, STR, and VTE). Heterogeneity and pleiotropy assessment was performed using Cochran's Q test, MR-Egger intercept test, and MR-PRESSO global test. For the deCODE QSOX2 pQTL data, post-GWAS annotation was performed with the FUMA platform to detect genomic risk loci and lead Single Nucleotide Polymorphisms (SNPs) and to carry out regional and functional annotation.[29] A *cis*-MR approach was then used to evaluate the direct genetic effect of plasma QSOX2 on CVD risk, and the SMR method was applied to assess causal relationships at the level of individual variants and to characterize the regulatory architecture.[30] All GWAS datasets were aligned to *GRCh37* using the LiftOver tool.[31] A detailed description of the data sources is provided in the Source Data. All datasets were publicly available, and ethical approval with informed consent had been obtained in the original studies.

Genetic Instrument Selection

Mendelian randomization analyses rely on 3 core assumptions: (1) the IVs are robustly associated with plasma QSOX1 or QSOX2; (2) the IVs are independent of potential confounders; (3) the IVs affect the risk of outcomes exclusively through the exposure.[32] The authors first excluded pQTLs with minor allele frequency of <0.01 or located on sex chromosomes or within the major histocompatibility complex region. Among the remaining pQTLs, genetic variants independently associated with QSOX1 or QSOX2 at genome-wide significance ($P < 5 \times 10^{-8}$) were identified after linkage disequilibrium (LD) clumping ($r^2 < 0.1$ within a 10 Mb window), consistent with the original pQTL study. When a selected SNP was unavailable in the outcome dataset, a proxy SNP in high LD ($r^2 > 0.8$) was used. Instrumental variables were then harmonized using

the R package "TwoSampleMR", and potential pleiotropic SNPs were removed by the R package "FastTraitR." Those excluded SNPs were in significant association ($P < 5 \times 10^{-8}$) with type 2 diabetes mellitus, *HbA1c* measurement, and low-density lipoprotein cholesterol measurement. The strength of the instruments was evaluated using the proportion of phenotypic variance explained (R^2) and *F*-statistics; only instruments with $F>10$ were retained to avoid weak-instrument bias. For the reverse MR analysis, genetic instruments for CVDs were defined as genome-wide significant SNPs ($P < 5 \times 10^{-8}$) after LD clumping ($r^2 <0.001$ within a 10 Mb window).

Mendelian Randomization Analyses

The inverse variance-weighted (IVW) method was used as the primary MR analysis.[33] Odds ratios (ORs) and 95% CIs were scaled to a 1-standard deviation (SD) increase in genetically predicted circulating QSOX1 or QSOX2 levels. Heterogeneity among individual SNP estimates was evaluated with Cochran's Q test.[34] Horizontal pleiotropy was assessed by the MR-Egger intercept test, and the MR-PRESSO global test was applied to detect and correct for pleiotropic outliers (requiring at least 4 SNPs).[35,36] The weighted median method was used as a sensitivity analysis.[37] For CVD outcomes that were nominally significant in the FinnGen screen, the authors performed fixed-effects meta-analyses combining FinnGen MR estimates with those from disease-specific consortia or GWAS summary reports. When heterogeneity across estimates was evident (Cochran's Q test $P <.05$), a random-effects model was used. All analyses were executed through the "Oneclick" pipeline integrating R packages "TwoSampleMR" and "MRPRESSO" in R version 4.5.1. *P*-value <.05 was considered statistically significant.

Mendelian Randomization Replication Analyses Using Whole or *cis* Region Protein Quantitative Trait Loci

Atrial fibrillation, HF, CHD, STR, and VTE were included in the MR replication analyses. The parameters and assessment of heterogeneity and pleiotropy were identical to those used in the primary MR analyses. *Pan*-MR analyses were performed using all IVs, whereas *cis*-MR analyses were restricted to IVs located within the *cis* region of *QSOX2*. In large-scale pQTL studies, the *cis* region is conventionally defined as extending 1 Mb on either side of the gene transcription start site (TSS).[38] To reduce potential *trans*-acting pleiotropy and better isolate direct protein effects, studies focusing on individual proteins or specific diseases often adopt a more stringent *cis* window ranging from 200 kb to 500 kb.[10,39] Accordingly, the authors defined the *cis* region as TSS ±500 kb. The *trans* region was defined as more than 5 Mb from the TSS, and the intervening region between 500 kb and 5 Mb was designated as *distal*. As sensitivity analyses, the authors performed: (1) MR using *distal* and *trans* region IVs; (2) *cis*-MR with a more stringent IV selection threshold ($r^2 <0.01$); (3) bidirectional MR to assess reverse causality using CVDs as the exposure and applying an $r^2 <0.001$ threshold. *P*-value <.05 was considered statistically significant.

Post-GWAS Annotation with FUMA

Post-GWAS regional and functional annotation was performed using FUMA (version 1.8.1), a web-based platform that integrates GWAS summary statistics with functional genomic resources to annotate, prioritize, and interpret genetic signals.[29] Using deCODE QSOX2 pQTL summary statistics as input, independent significant SNPs were first identified by applying a clumping procedure with a genome-wide significance threshold of $P <5 \times 10^{-8}$ and an LD threshold of $r^2 <0.6$ against the 1000 Genomes Project Phase 3 reference panel. Lead SNPs were then defined by a second round of clumping among the independent significant SNPs at a more stringent threshold of $r^2 <0.1$. Genomic risk loci were constructed by merging lead SNP-associated LD blocks if they were separated by less than 250 kb. Within each risk locus, all SNPs in LD ($r^2 \geq 0.6$) with any of the independent significant SNPs were compiled into a candidate SNP set. This set therefore includes independent significant SNPs themselves and their LD proxies, including those absent from the original GWAS input. Functional annotation of all candidate SNPs was performed to ensure comprehensive coverage of potentially causal variants. The resulting lists of independent significant SNPs, lead SNPs, genomic risk loci, and candidate SNPs were used to characterize the pQTL architecture of QSOX2 and to guide downstream prioritization of causal variants.

Causal Variant Prioritization

To prioritize likely causal variants for QSOX2, the authors integrated pQTL significance, position within the *QSOX2* region, and functional annotations provided by FUMA. Independent significant SNPs and their LD proxies (candidate SNPs) in the coding region were annotated using ANNOVAR to determine their functional consequences (e.g., nonsynonymous, stop-gain, and intergenic).[40] The Combined Annotation Dependent Depletion (CADD) framework employs a support vector machine trained to distinguish variants that have become fixed in human populations from simulated de novo mutations.[41] By integrating over 60 genomic and epigenomic annotations, it generates a single C-score for each variant; a C-score≥12.37 was considered indicative of a damaging effect.[42] The RegulomeDB score (categorical scale 1a-7, where 1a represents the strongest evidence for regulatory function) was used to evaluate regulatory DNA elements.[43] Expression quantitative trait loci (eQTL) annotations were extracted from the FUMA output, which are based on publicly available *cis* eQTL datasets to identify SNPs significantly associated with *QSOX2* expression across tissues. Among the prioritized causal variants, the missense mutation *rs12380852:C* (*g.139118673T>C*, *c.376A>G*, *p.Lys126Glu*) emerged as the top candidate. Structural assessment was performed using the AlphaFold-predicted model of QSOX2 available through the Open Targets Platform (https://platform.opentargets.org/variant/9_136226827_T_C), which localizes the K126 residue within the thioredoxin domain and supports the plausibility of the substitution altering domain stability and/or catalytic activity.[44,45]

Summary-Data-Based Mendelian Randomization Analyses of cis and trans Protein Quantitative Trait Loci

The SMR method is designed to identify causal genes or proteins underlying disease-associated loci. Summary-data-based Mendelian randomization analyses in this study's

case were conducted using the SMR software tool (version 1.4.0) at the command line with default parameters, testing whether the effect of a genetic variant on a CVD outcome was mediated by genetically regulated QSOX2 levels.[30] The Heterogeneity in Dependent Instruments (HEIDI) test was then applied to distinguish whether the protein-disease association was driven by the same causal variant (vertical pleiotropy) or by distinct variants in LD. For *trans*-acting pQTLs of QSOX2, significant SMR associations with a HEIDI $P > .05$ may reflect regulatory interactions or networks between the gene products at the *trans* locus and QSOX2 that jointly influence CVD risk. False discovery rate (FDR) correction was applied across SMR analyses using the Benjamini–Hochberg method, with FDR <0.10 considered statistically significant.

RESULTS

Association of Genetically Predicted Circulating QSOX1 or QSOX2 Levels with Cardiovascular Disease Outcomes in the FinnGen Dataset Screen

An overview of the study design is shown in Figure 1. INTERVAL pQTL and FinnGen disease data were applied for the preliminary analysis. The authors identified 4 and 26 valid SNPs as genetic instruments for circulating QSOX1 and QSOX2 levels, respectively (all F-statistics >10, Supplementary Tables 1 and 2). In IVW MR analysis, genetically predicted levels of circulating QSOX1 were positively associated with the risk of STR (Supplementary Figure 1). For QSOX2, genetically predicted higher levels were associated with increased risks of AF, CHD, HF, STR, IS, and VTE (Figure 2). Sensitivity analyses using weighted median and MR-Egger methods confirmed the direction of these associations (Supplementary Tables 3 and 4). Cochran's Q test indicated evidence of IV heterogeneity in the analyses of AF, CHD, HF, IS, and VTE. All analyses passed the MR-Egger intercept test for horizontal pleiotropy. Although MR-PRESSO analysis identified several outliers, the effect estimates remained largely unchanged after their removal, except in the AF analysis using the Nielsen et al's[24] dataset (Supplementary Table 5).

For CVD outcomes that showed nominal significance in the FinnGen screen, the authors conducted further meta-analyses that pooled MR estimates from FinnGen with those from disease-specific consortia or GWAS summary datasets. Each 1-SD increase in genetically predicted QSOX1 levels was associated with a decreased risk of VTE (OR = 0.96,

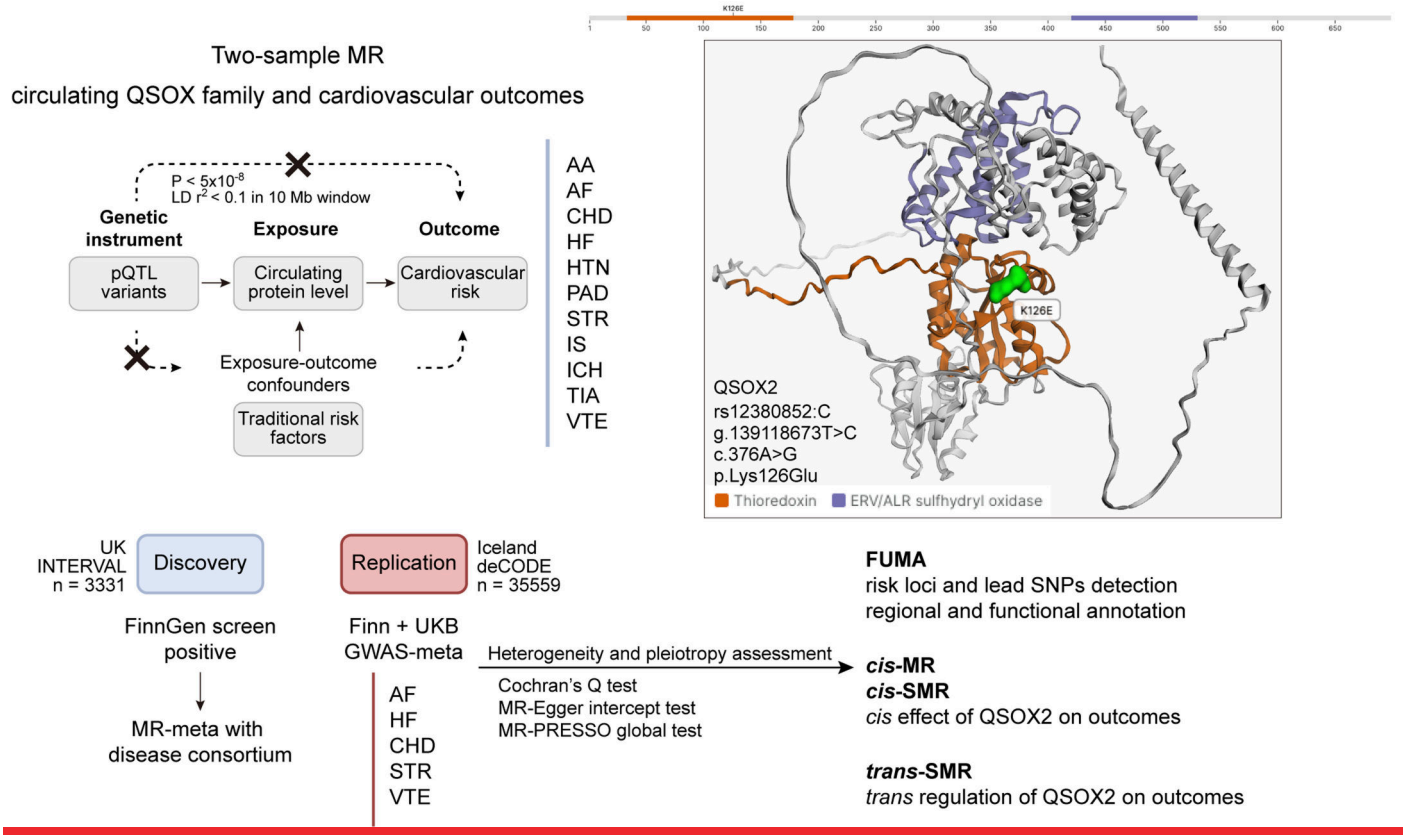


Figure 1. Study design overview. The study employed a 2-sample MR design integrated with post-GWAS annotation. In the discovery stage, INTERVAL pQTLs were combined with FinnGen disease outcomes; nominally significant results were then meta-analyzed with independent disease-specific consortia. Replication analyses used deCODE pQTLs together with GWAS data from the FinnGen–UKB meta-analysis. Post-GWAS annotation with FUMA identified genomic risk loci and lead SNPs to guide causal variant prioritization. Cis-MR and SMR were subsequently applied to evaluate direct causal effects and to characterize the cis/trans regulatory architecture. Structural assessment of *rs12380852* was performed using the AlphaFold-predicted model of QSOX2 available through the Open Targets Platform. MR, Mendelian randomization; PQTLs, protein quantitative trait loci; SMR, summary-data-based Mendelian randomization; UKB, UK Biobank.

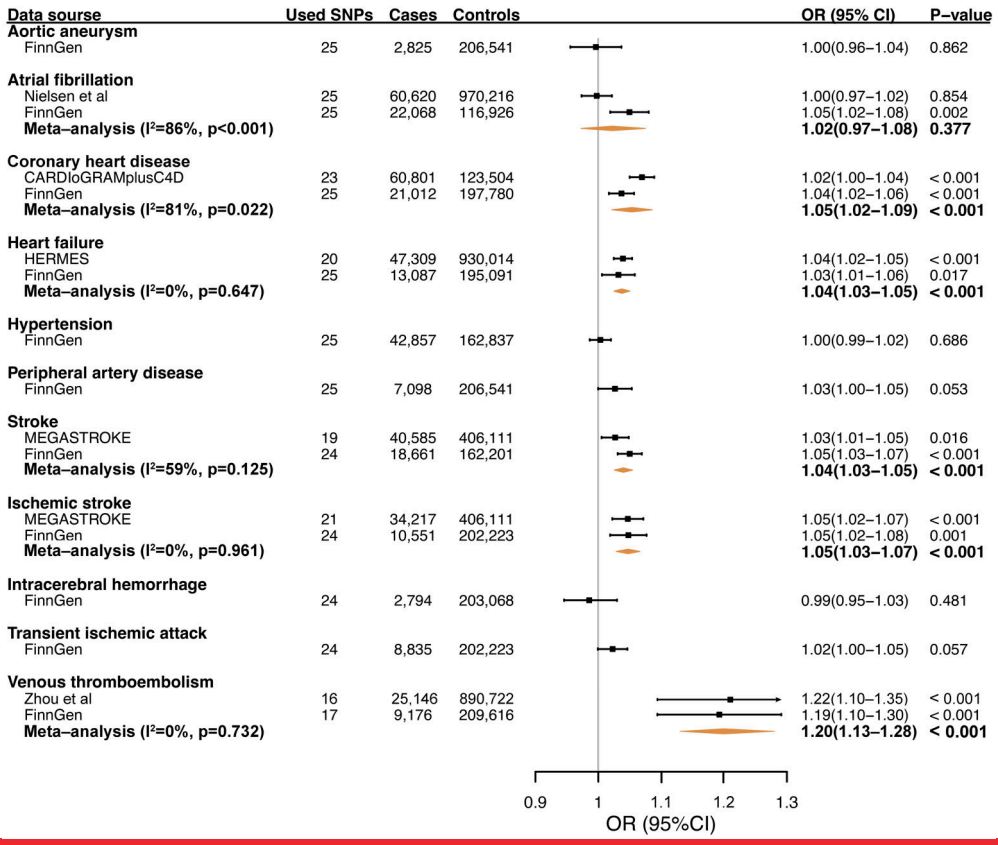


Figure 2. Screening of associations between genetically predicted circulating QSOX2 levels and CVD risk. MR estimates for the effect of circulating QSOX2 on various cardiovascular outcomes are shown, derived from INTERVAL pQTL data and FinnGen GWAS plus disease-specific consortia. Results are displayed as ORs with 95% CIs. CVD, cardiovascular disease; MR, Mendelian randomization; pQTL, protein quantitative trait locus.

P = .033, 95% CI: 0.93-0.99, Supplementary Figure 1), whereas the association with STR was attenuated and no longer significant after meta-analysis (OR = 1.02, *P* = .693, 95% CI: 0.94-1.10). For QSOX2, the meta-analyses confirmed consistent risk-increasing associations with CHD (OR = 1.05, *P* <.001, 95% CI: 1.02-1.09, Figure 2), HF (OR = 1.04, *P* <.001, 95% CI: 1.03-1.05), STR (OR = 1.04, *P* <.001, 95% CI: 1.03-1.05), IS (OR = 1.05, *P* <.001, 95% CI: 1.03-1.07), and VTE (OR = 1.20, *P* <.001, 95% CI: 1.13-1.28). In contrast, the association between QSOX2 and AF was attenuated and became non-significant in the meta-analysis (OR = 1.02, *P* = .377, 95% CI: 0.97-1.08).

SNP-Level Heterogeneity in Mendelian Randomization Analyses

To validate the preliminary findings of this study, the authors further leveraged newly released, larger GWAS summary data. The UK Biobank Pharma Proteomics Project (UKB-PPP) measured 2920 proteins in 53 026 individuals, including QSOX1. A comprehensive atlas based on these data reported epidemiological and genomic associations of these proteins with common phenotypes and diseases.[46] While QSOX1 exhibited positive epidemiological correlations with various incident or prevalent CVD outcomes, including STR, none of these associations were supported by MR analysis (see Source Data). For QSOX2, the deCODE study provided high-quality pQTL data from 35 559 participants, covering 4907 proteins. By integrating deCODE pQTLs with disease GWAS data from a FinnGen–UKB meta-analysis, the authors replicated MR analyses for AF, CHD, HF, STR, and VTE. The direction of effect estimates for QSOX2 remained risk-increasing; however, all analyses exhibited significant heterogeneity according to Cochran's Q test (Figure 3A).

The authors next compared the genetic instruments identified in the INTERVAL and deCODE studies. The deeper sequencing coverage of deCODE enabled the discovery of additional pQTLs beyond chromosome 9 (Figure 3B). Given that *cis* pQTLs are more likely to reflect direct protein effects on disease, whereas *trans* pQTLs may reflect underlying mechanisms, the authors focused on the deCODE data and performed post-GWAS annotation using the FUMA platform to delineate *cis* regions and *cis*-acting IVs. Independent significant SNPs and their surrounding genomic risk loci were identified based on LD structure, after which lead SNPs and candidate SNPs were selected. FUMA identified 339 lead SNPs derived from 807 independent significant SNPs, distributed across 12 genomic risk loci. Consistent with the location of the QSOX2-coding sequence on chromosome 9, the majority of pQTLs mapped to a single genomic risk locus on chromosome 9 (*Chr9:132978862-141104560*; spanning 8.13 Mb; Figure 3B). This dense QTL region contained 4951 candidate SNPs that were in LD with independent significant

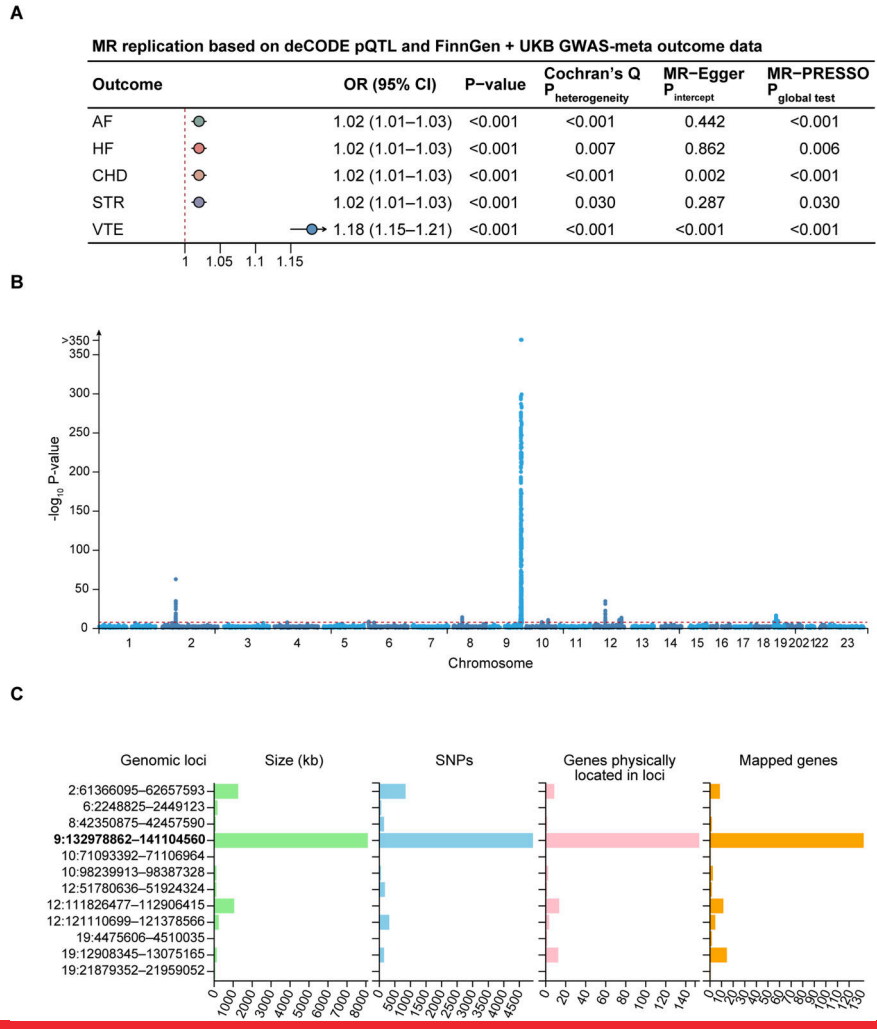


Figure 3. Validation of MR results and annotation of pQTL data. (A) Forest plot showing replication of MR results for the effect of circulating QSOX2 on CVDs, using larger GWAS summary data. Genetic instruments for QSOX2 were derived from the deCODE study (pQTL data), and outcome data for CVDs were obtained from a FinnGen–UKB meta-analysis. (B) Manhattan plot of the deCODE QSOX2 pQTL data. The x-axis represents chromosomal position, and the y-axis represents the $-\log_{10}$ *P*-value for SNP associations with circulating QSOX2 levels. The red dotted line indicates the genome-wide significance threshold ($P < 5\times10^{-8}$). (C) Histograms summarizing the genomic risk loci identified by FUMA from the deCODE QSOX2 pQTL summary statistics.CVDs, cardiovascular disease; MR, Mendelian randomization; pQTL, protein quantitative trait locus; UKB, UK Biobank.

SNPs, identified from both the deCODE dataset and the 1000 Genomes reference panel. These candidate SNPs mapped to 154 prioritized genes, 133 of which were identified in the deCODE dataset (Figure 3C).

Protein Quantitative Trait Locus Architecture and Prioritized Causal Variants for Circulating QSOX2

Within the chromosome 9 genomic risk locus, the authors observed 2 distinct peaks: one centered at approximately 136 Mb and the other at 139 Mb (Figure 4A). Given that *cis* regions are conventionally defined as ±500 kb to ±1 Mb around the gene TSS, the authors focused on the 139 Mb region. The 136 Mb region, which lies between the *cis* and *trans* boundaries, was designated as *distal*. Post-GWAS annotation further enabled the prioritization of potential causal variants, a critical step for the biological interpretation of GWAS signals and the design of subsequent experimental validation. Within the QSOX2-coding sequence in the *cis* region, the authors identified 1 lead SNP and 4 independent significant SNPs (Figure 4B) whereas the lead SNP (*rs10858248*) is located in an intergenic region, 2 of the independent significant SNPs are exonic. Of those, the missense variant *rs12380852* at position 139118673 in exon 2 represents the most plausible causal candidate (Figure 4C). This variant corresponds to a T>C substitution, resulting in a *p.Lys126Glu* (K126E) missense mutation. Integration of CADD scores, RegulomeDB scores, and eQTL mapping evidence suggests that *rs12380852* is a functionally damaging variant likely to alter QSOX2 protein levels and/or activity by affecting protein structure rather than transcriptional or epigenetic regulation.

Cis and *Trans* Regulation of Circulating QSOX2 in Cardiovascular Diseases

The authors next performed *cis*-MR analyses using 33 *cis* pQTLs as IVs (Supplementary Table 6). The results revealed negative associations of circulating QSOX2 with AF

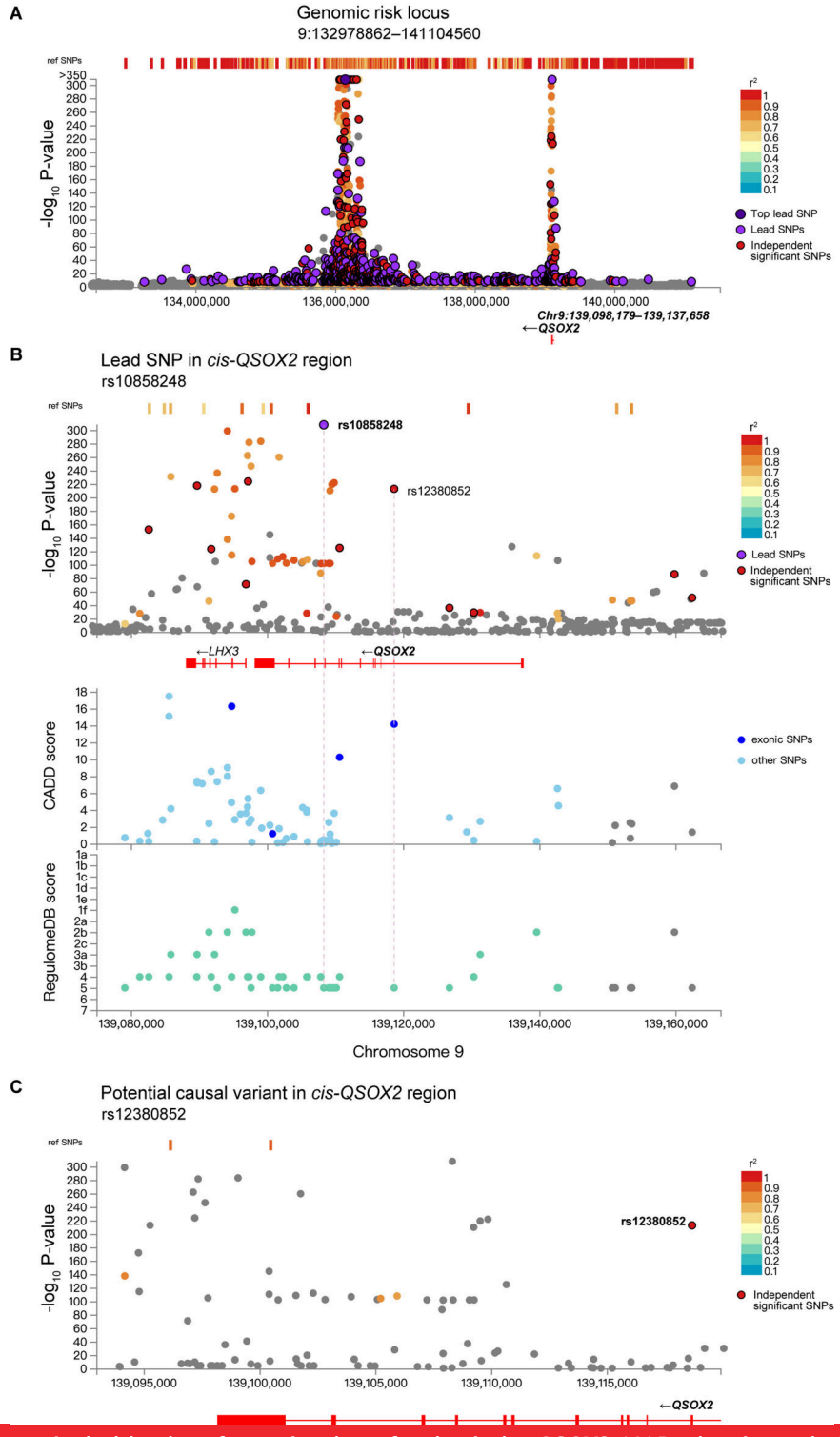


Figure 4. Fine-mapping and prioritization of causal variants for circulating QSOX2. (A) Regional association plot of the genomic risk locus on chromosome 9, showing SNP associations with circulating QSOX2 levels. The top lead SNP (*rs550057*) is highlighted in dark purple, with other lead SNPs shown in purple and independent significant SNPs in red. Additional SNPs are colored based on their LD (r2) with independent significant SNPs. (B) Regional association plot of the lead SNP (*rs10858248*) in the cis-QSOX2 region, annotated with CADD scores and RegulomeDB scores to indicate SNP functional importance. *rs10858248* is highlighted in purple, and independent significant SNPs are shown in red. Additional SNPs are colored based on their LD with independent significant SNPs. (C) Regional association plot focusing on the potential causal SNP (*rs12380852*) in the cis-QSOX2 region. SNPs are colored based on their LD with *rs12380852*. Non-GWAS-tagged SNPs in the 1000G reference panel that are in LD with the specific SNP in A-C are shown at the top of each plot as rectangles. CADD, Combined Annotation–Dependent Depletion.

(OR = 0.96, *P* = .007, 95% CI: 0.94-0.99) and HF (OR = 0.95, *P* <.001, 95% CI: 0.93-0.97, Figure 5A), with no evidence of IV heterogeneity or horizontal pleiotropy. These seemingly protective roles are opposite to the *pan*-MR results. The authors noted that the pQTLs from both the INTERVAL and deCODE datasets were primarily located in the 136 Mb *distal* region (Supplementary Table 2 and Figure 4A). Mendelian randomization analyses using these *distal* IVs yielded positive associations with disease outcomes (see Source Data), suggesting that *distal* variants may confound the *pan*-MR results. To further evaluate *cis* and *trans* effects at the individual QTL level and to facilitate biological and mechanistic interpretation,

A

***cis*-MR (*cis* region defined as TSS ± 500kb)**

Outcome	OR (95% CI)	P-value	Cochran's Q $P_{heterogeneity}$	MR-Egger $P_{intercept}$	MR-PRESSO $P_{global\ test}$
AF	0.96 (0.94–0.99)	0.007	0.209	0.012	0.221
HF	0.95 (0.93–0.97)	<0.001	0.888	0.060	0.895
CHD	1.00 (0.98–1.03)	0.792	0.326	0.008	0.279
STR	0.99 (0.95–1.02)	0.500	0.002	0.406	0.003
VTE	1.00 (0.97–1.03)	0.991	0.051	0.110	0.061



B

***cis*-SMR (Chr9 rs12380852:C *QSOX2* exon2 missense variant)**

Outcome	OR (95% CI)	P-value	FDR	P-HEIDI
AF	0.93 (0.88–0.98)	0.009	0.044	0.125
HF	0.94 (0.90–0.99)	0.040	0.066	0.734
CHD	1.01 (0.96–1.05)	0.696	0.696	0.187
STR	0.96 (0.90–1.02)	0.196	0.245	0.053
VTE	0.93 (0.89–0.99)	0.030	0.066	0.122

C

D

***trans*-SMR (Chr12 rs3184504:C *SH2B3* exon2 missense variant)**

Outcome	OR (95% CI)	P-value	FDR	P-HEIDI
AF	1.86 (1.35–2.53)	<0.001	0.002	0.685
HF	1.79 (1.32–2.44)	<0.001	0.002	0.635
CHD	3.67 (2.36–5.70)	<0.001	<0.001	0.254
STR	2.03 (1.45–2.86)	<0.001	<0.001	0.550
VTE	2.36 (1.63–3.46)	<0.001	<0.001	0.961

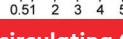


Figure 5. Cis and trans regulation of circulating QSOX2 pQTLs on CVD outcomes. (A) Forest plot of cis-MR results showing the associations of circulating QSOX2 with CVDs using cis-acting variants as instruments. (B) Forest plot of cis-SMR results for the prioritized causal variant *rs12380852*. (C) Scatter plot displaying significant cis and trans pQTLs of QSOX2 associated with CVD outcomes, as evaluated by SMR and HEIDI tests. Each point represents a single variant, with coordinates corresponding to its effect size (with 95% CIs) on circulating QSOX2 levels (exposure, x-axis) and on CVD risk (outcome, y-axis). The first appearance of the same pQTLs in a row is labeled with its rsID and mapped gene. (D) Forest plot of trans-SMR results for *rs3184504*, a missense variant in SH2B3, showing the estimated effect of the trans pQTL for QSOX2 on cardiovascular outcomes.CVD, cardiovascular disease; HEIDI, Heterogeneity in Dependent Instruments; MR, Mendelian randomization; pQTLs, protein quantitative trait loci; SMR, summary-data-based Mendelian randomization.

the authors applied the SMR method. Consistent with the *cis*-MR findings, *cis*-SMR analysis for the *cis* pQTL *rs12380852* showed that plasma QSOX2 was negatively associated with AF (OR = 0.93, *P* = .009, 95% CI: 0.88-0.98, Figure 5B) and HF (OR = 0.94, *P* = .040, 95% CI: 0.90-0.99). The HEIDI test supported *rs12380852* as a causal variant underlying the protective role of QSOX2 against AF and HF. The lead SNP in the *cis* region, *rs10858248*, also exhibited protective associations with these outcomes (Figure 5C). Additionally, VTE was identified as another protective outcome associated with the QSOX2 *cis* pQTL *rs12380852* (OR = 0.93, *P* = .030, 95% CI: 0.89-0.99).

The deCODE dataset also contained a number of *trans*-acting pQTLs. The authors therefore extended the SMR analyses to *trans* pQTLs to explore potential regulatory pathways linking QSOX2 to CVDs. The analyses identified several pleiotropic variants that influence both QSOX2 protein levels and CVD risk, as supported by SMR and HEIDI tests (see Source Data). The variants are *rs3184504* (located in the gene region of *SH2B3*), *rs8887* (*HDGFRP2*), *rs9392385* (*GMDS-AS1*), *rs2923444* (*SLC20A2*), and *rs6511291* (*ZNF100*). Interestingly, the direction of *trans* pQTL associations was largely opposite to that of the *cis* pQTL effects. Among these *trans*-acting variants, *rs3184504* showed significant positive associations with all 5 CVD outcomes; *rs6511291* was positively associated with all outcomes except VTE; *rs8887* was positively associated with AF; *rs9392385* was positively associated with CHD; whereas *rs2923444* exhibited a negative association with CHD (Figure 5C). The authors selected *rs3184504* for detailed characterization (Figure 5C and 5D). *rs3184504* is a missense variant in *SH2B3*, which encodes the *SH2B* adapter protein 3, a key negative regulator of inflammatory signaling in CVDs. The CC-encoding allele (the effect allele in this study's pQTL analysis) helps preserve the anti-inflammatory function of *SH2B3*. Identified as both a *trans* pQTL for QSOX2 and a missense variant of *SH2B3*, the *trans*-SMR results suggest that when *SH2B3*-mediated inflammatory restraint is intact, CVD risk is low and QSOX2 remains quiescent. This interpretation aligns with the established role of QSOX2 in maintaining systemic homeostasis and protein folding integrity.

DISCUSSION

In this study, the authors assessed the causal association of circulating QSOX family enzymes with CVD risk by integrating MR and post-GWAS analyses. The results of this study provide genetic evidence that QSOX2 levels in human blood are associated with multiple CVD outcomes, and these associations were validated using larger GWAS datasets. To resolve the observed SNP-level heterogeneity, the authors annotated the deCODE pQTL data for QSOX2, prioritized causal variants, and dissected the divergent contributions of *cis* and *trans* pQTLs to CVD susceptibility.

Notably, the missense variant *rs12380852* emerged as a likely causal candidate, either alone or in combination with other *cis*-acting variants, suggesting that circulating QSOX2 may protect against AF and HF. This favorable effect may be mediated through its canonical function in stabilizing disulfide bonds in the ECM, as well as by preserving proteostasis and cellular homeostasis under inflammatory conditions. Collectively, the findings of this study support a protective role of circulating QSOX2 in AF and HF, and the causal variants identified here may serve as targets for future functional validation and druggable design.

The QSOX family of flavoproteins catalyzes disulfide bond formation with the concurrent reduction of oxygen to hydrogen peroxide, either within the Golgi apparatus or in the extracellular space. Disulfide bonds are indispensable for the structural and functional integrity of numerous proteins involved in CVDs. However, no systematic evaluation has yet been conducted to assess the causal role of circulating QSOX enzymes in CVDs. The authors therefore performed a screen using pQTL data for QSOX1 and QSOX2 from the INTERVAL study and CVD outcomes from FinnGen (release R5), followed by meta-analyses with non-overlapping disease-specific consortia for nominally significant results. The preliminary analyses suggested associations of circulating QSOX1 with STR and VTE, and of QSOX2 with CHD, HF, AF, STR (including ischemic stroke), and VTE. The application of protein-based MR has been constrained by the limited availability of suitable genetic instruments, particularly for QSOX1 in this study's case, which may introduce bias or reduce statistical power. The authors therefore sought validation in larger datasets. The UKB-PPP characterized thousands of plasma proteins and their pQTLs using the Olink platform, and a subsequent atlas research systematically profiled the genomic and epidemiological associations of these proteins, including QSOX1 (https://proteome-phenome-atlas.com). Plasma QSOX1 was reported to be positively associated with various prevalent and incident CVDs (e.g., STR, VTE, HTN, AF, and HF), but no causal evidence was confirmed using *cis*-MR analyses with up to 24 IVs (e.g., AF and HF), and analyses of reverse causality were likewise null. The null MR results suggest QSOX1 may serve more as a disease marker than as a causal contributor, while the authors cannot completely rule out residual confounding in observational studies, reverse causality, and non-linear effects. Interestingly, QSOX1 has been found to be upregulated in the heart of mice and rats and in human blood during acute decompensated heart failure, and QSOX1$^{-/-}$ mouse hearts exhibited chronic endoplasmic reticulum stress and dilated cardiomyopathy.[12,47] With respect to HTN, a recent study uncovered a role for beige fat-secreted QSOX1 in vascular fibrosis and constriction via adipocyte-vascular crosstalk, through catalyzing disulfide bond formation on angiotensin receptors of smooth muscle cells and on ECM proteins.[11] Given these experimental data, the authors further infer that QSOX1 may function more as a local mediator in cell-cell communication within the heart or vasculature, and that elevated circulating QSOX1 levels may primarily reflect active regulatory processes in the tissue microenvironment rather than directly contributing to systemic CVD risk.

SomaScan represents another reliable high-throughput proteomic platform, adopted by both the INTERVAL and deCODE studies. The authors therefore repeated MR analyses using deCODE pQTLs for plasma QSOX2 and CVD outcomes from

a FinnGen—UKB meta-analysis GWAS resource. This analysis included over 200 IVs and showed pronounced heterogeneity and pleiotropy. To dissect the sources of heterogeneity, the authors fine-mapped the pQTL data and performed *cis*-MR to reduce pleiotropic effects, a strategy that has become standard in post-GWAS proteogenomic studies. Using the FUMA platform, the authors re-annotated the pQTL data. Although the *QSOX2* TSS lies within the identified genomic risk locus on chromosome 9 (139 Mb), the top lead pQTL signal mapped to 136 Mb, beyond the conventional *cis* window. Large-scale pQTL studies commonly define the *cis* region as TSS ±1 Mb, whereas disease-focused investigations often adopt narrower windows.[48,49] The authors initially applied a 1 Mb window but still observed notable residual pleiotropy (see Source Data), and therefore defined *cis* as ±500 kb from the TSS, *trans* as >5 Mb, and the intervening region as *distal*. Up to 42 valid SNPs (r^2 <0.1) were included in the *cis*-MR analysis, which indicated that plasma QSOX2 may exert a protective effect on AF and HF with no evidence of heterogeneity or pleiotropy. Consistent results were obtained with a more stringent instrument selection (9 SNPs, r^2 <0.01, see Source Data). Additionally, no evidence supported reverse causality (see Source Data). Two previous MR studies, both using deCODE pQTL data combined with disease outcomes from the Nielsen et al[24] meta-analysis, also reported a protective association of QSOX2 with AF, employing 3 and 1 *cis* pQTLs as instruments, respectively.[39,50] In the prospective AGES-Reykjavik study, which integrated genomic and proteomic data from 4765 individuals, 2 *cis* IVs likewise linked higher circulating QSOX2 levels to reduced incident AF risk, although no epidemiological association was detected.[10] Compared with these studies, the authors' analysis incorporated a larger number of *cis* IVs, thereby improving statistical power. Moreover, the use of GWAS summary statistics from independent, non-overlapping cohorts for exposure and outcome helped mitigate the risk of false-positive MR findings.

The authors next examined the *distal* and *trans* regions using MR. *Trans*-MR results were null, whereas the 136 Mb *distal* region showed positive associations with diseases (see Source Data), consistent with the *pan*-MR estimates but opposite to the direction observed in *cis*-MR. This region contributed 77.8% of the IVs and exhibited SNP-level heterogeneity, indicating that the risk-increasing signals observed in the *pan*-MR analysis were primarily driven by confounding through these *distal* variants. The *distal* and *trans* regions the authors defined harbor *trans*-acting variants that may affect multiple phenotypes simultaneously, leading to pleiotropy. Although the authors cannot completely exclude long-range *cis* regulation of QSOX2, the 136 Mb region encompasses the *ABO* gene (the top lead SNP rs550057 is an eQTL for ABO), a well-established *trans* pQTL hotspot known to associate with multiple cardiovascular traits and to exert widespread pleiotropic effects.[51] Interestingly, a previous pQTL study of AF identified the *cis* pQTL *rs10858248* as a candidate causal variant conferring the protective effect of QSOX2 on AF through colocalization analyses, but this finding failed to replicate in the Fenland study, where the opposite effect direction was observed.[49] Notably, the single variant *rs115478735* that they selected for SMR and colocalization analyses, chosen solely on the basis of minimal *P*-value, maps to the 136 Mb *distal* region. Taken together, the authors' *cis*-MR findings align with previous reports of a protective effect of plasma QSOX2 on AF and newly extend this favorable role to HF, while the *distal* region emerges as the principal source of heterogeneity and pleiotropy in the *pan*-MR analyses.

As *cis* regulation pointed to a protective role of QSOX2, post-GWAS annotation further enabled the selection of likely causal variants over merely associated signals and facilitated inference of their *cis*- or *trans*-acting roles in CVDs. Zooming into the QSOX2-coding region, the authors identified a protein-altering variant among the pQTL candidates—*rs12380852:C*. QSOX2 catalyzes disulfide bond formation via interdomain disulfide exchanges that relay reducing equivalents from substrates to the flavin cofactor and ultimately to molecular oxygen.[52,53] The *rs12380852* variant causes a lysine-to-glutamic acid substitution at position 126 (K126E) within the N-terminal thioredoxin domain that participates in the initial steps of this electron relay. This substitution is predicted to disrupt local electrostatic interactions and interdomain electron transfer, likely compromising the structural stability and enzymatic activity of QSOX2. By integrating available functional annotations, including predicted variant deleteriousness (CADD scores), potential regulatory elements (RegulomeDB scores), and effects on gene expression (eQTL mapping data), the authors pinpointed *rs12380852* as a likely causal variant that may act by lowering total circulating QSOX2 levels and/or by impairing protein function. It is noteworthy that genetic variants altering protein structure can generate apparent *cis* pQTL signals through aptamer-binding artifacts rather than true quantitative differences in protein abundance, particularly when *cis* pQTLs lack corresponding *cis* eQTLs.[15] However, the observed moderate effect size of *rs12380852* on circulating QSOX2 levels, rather than an extreme loss of signal (see Source Data), is considered to carry a higher biological prior probability. Interestingly, the lead SNP *rs10858248* in the *cis* region represents another causal candidate, as it is in high LD (r^2 = 0.85) with *rs3780190*, a known eQTL for *QSOX2* located in the 3′ UTR, which may influence mRNA stability and translational efficiency, thereby affecting protein abundance.

For the prioritized causal variants, the authors further applied the SMR method to assess whether the pQTL and disease GWAS signals share a common causal variant, and whether QSOX2 acts as a functional effector connecting genetic variants to disease. Both *rs12380852* and *rs10858248* were associated with lower circulating QSOX2 abundance and higher risk of AF and HF, and *cis*-SMR analyses supported QSOX2 as a causal mediator at this locus. To date, few experimental studies have directly investigated the causal role of QSOX2 in CVDs. Given that the secreted homolog QSOX1 is essential for laminin incorporation into the ECM, QSOX2 may similarly promote ECM assembly, thereby maintaining cardiac structural and signaling homeostasis, preventing adverse remodeling and fibrosis, and consequently

protecting against AF and HF.[54-56] Additionally, when localized to the nuclear membrane, QSOX2 has been reported to act as a "gatekeeper" enabling body growth and preserving mitochondrial integrity by modulating the growth hormone–STAT5B axis.[57]

Beyond *cis* regulation, this study's *trans*-SMR analyses uncovered potential regulatory networks linking QSOX2 to CVDs. Among the *trans*-acting variants identified, *rs3184504* was particularly informative. This variant is a well-characterized missense polymorphism in *SH2B3*.[58] It was identified as both a *trans* pQTL for QSOX2 and a *cis* eQTL for *SH2B3*, and colocalized with risk of AF, HF, CHD, STR, and VTE.[59-63] *SH2B3* encodes the *SH2B* adapter protein 3 (LNK), which serves as a key negative regulator of cytokine signaling, inflammation, and oxidative stress, primarily by restraining JAK–STAT signaling.[64] The *rs3184504* missense variant modulates SH2B3 function, and its CC-encoding allele confers protection against multiple cardiovascular and autoimmune conditions through preserved anti-inflammatory property.[65-69] This study's *trans*-SMR analyses recognized QSOX2 as an effector linking *rs3184504* to disease traits, probably secondary to the primary effect of *SH2B3* on cardiovascular risk. When *SH2B3*-mediated inflammatory control is impaired, systemic inflammation drives upregulation of QSOX2 as an endoplasmic reticulum stress- and redox-sensitive protein, which may be captured as a coincident *trans* signal but should not be interpreted as evidence of direct pathogenicity. Thus, the *trans*-SMR findings for *rs3184504* point to the *SH2B3*–inflammatory axis as a likely upstream regulator of QSOX2 and underscore the importance of distinguishing *trans*-acting signals when interpreting protein-to-disease MR results, as they may reflect upstream pleiotropic pathways rather than direct protein effects.

Study Limitations

Despite the strengths of this study, several limitations should be considered. First, although the authors adopted *cis*-MR analyses to reduce horizontal pleiotropy, residual confounding from transcriptional, post-transcriptional, or LD-related mechanisms may still obscure a direct protein-to-disease causal relationship. Second, the genetic instruments for plasma QSOX1 and QSOX2 in the INTERVAL study may be insufficient or suboptimal, which gave rise to limited statistical power and SNP-level heterogeneity in the initial screen. To address these issues, the authors employed a comprehensive strategy to validate the causal contribution of QSOX2 to CVDs and to characterize its genetic architecture, thereby reducing the impact of instrument limitations. Third, this study populations were predominantly of European ancestry, which limits the generalizability of these findings to other ethnic groups. This concern is particularly relevant to the functional variants the authors characterized: both *rs12380852:C* and *rs3184504:C* exhibit notable allele frequency discrepancies between European and East Asian populations. Multi-ancestry MR studies will be helpful for verifying cross-population consistency or uncovering population-specific biological mechanisms. Fourth, the modest effect sizes observed in this study reflect a recognized issue in MR analyses of proteins. Because the processing of protein GWAS data (such as rank-inverse normal transformation) precludes direct clinical interpretation of MR OR values, the authors focused on the direction and consistency of effects rather than their magnitude.[14,39] Importantly, the reliable demonstration of even a modest causal effect remains informative, as it can pinpoint a biomarker that may predict disease risk and guide interventions that produce a much larger effect on the same protein in population-based studies. Fifth, although QSOX2 can be reliably and conveniently measured in plasma, the relevance of these systemic concentrations to local protein activity in cardiac or vascular tissues remains uncertain. Further assessment of tissue- or cell-specific QSOX2 expression and function may provide deeper insights into disease pathophysiology. Lastly, this study is limited by its reliance on in silico approaches. The authors' analyses suggested a protective role of QSOX2 in CVDs and inflammation, with *rs12380852* (*K126E*) prioritized as a causal variant. Given that QSOX2 has been listed as a druggable target by others, experimental validation is still required to substantiate these findings and to confirm the proposed causal variant.[70] For instance, future studies should biochemically characterize the enzymatic activity of the *K126E* mutant, examine whether QSOX2 depletion or overexpression alters ECM organization and fibrosis in cardiac models of AF and HF, and test whether modulating QSOX2 levels affects the SH2B3–JAK–STAT inflammatory cascade in vascular or myocardial tissues.

CONCLUSIONS

In conclusion, this integrative MR and post-GWAS study provides genetic evidence that circulating QSOX2 protects against AF and HF, supported by dissection of its *cis*- and *trans*-regulatory architecture. Future experimental validation of the prioritized causal variant and the implicated inflammatory pathways is warranted to translate these genetic insights into therapeutic opportunities.

Artificial intelligence (AI) assistance declaration: The authors did not use any AI-assisted technologies in the creation of this manuscript.

Ethics Committee Approval: All GWAS datasets used in this study were publicly available, and ethical approval was obtained in each of the original studies.Informed Consent: All GWAS datasets used in this study were publicly available, and informed consent was obtained in each of the original studies.Peer-review: Externally peer-reviewed.

Author Contributions: Conception – Z.C., J.Q.; Design – Z.C., J.Q.; Supervision – J.G.; Resource – Y.X., Z.Y., X.S.; Materials – Y.X., Z.Y., X.S.; Data Collection – X.C., Y.X.; Analysis and interpretation – X.C., A.C.; Literature Search – X.C., A.C., B.Y., D.L., J.M.; Writing – X.C., A.C.; Critical Reviews – Z.C., J.Q. All authors read and approved the final manuscript.

Declaration of Interests: The authors have no conflicts of interest to declare.

Funding: This study was supported by the National Program on Key Basic Research Project of China (grant number 2023YFC2506500, 2022YFC2407002); National Natural Science Foundation of China

(grant number 82470338, T2288101, 82170338); Open research Subject No.15 fund of State Key Laboratory of Cardiovascular Diseases; Shanghai Municipal Key Clinical Specialty (grant number shslczdzk01701); Grant of Shanghai Municipal Health Commission (grant number 2022JC012); Grant of Zhongshan Hospital Affiliated to Fudan University (grant number 2023ZSFZ43).

REFERENCES

1. GBD 2021 Causes of Death Collaborators. Global burden of 288 causes of death and life expectancy decomposition in 204 countries and territories and 811 subnational locations, 1990-2021: a systematic analysis for the Global Burden of Disease Study 2021. *Lancet*. 2024;403(10440):2100-2132. [CrossRef]
2. Qian S, Chen G, Li R, et al. Disulfide stress and its role in cardiovascular diseases. *Redox Biol*. 2024;75:103297. [CrossRef]
3. Barallobre-Barreiro J, Lynch M, Yin X, Mayr M. Systems biology-opportunities and challenges: the application of proteomics to study the cardiovascular extracellular matrix. *Cardiovasc Res*. 2016;112(3):626-636. [CrossRef]
4. Hall C. Essential biochemistry and physiology of (NT-pro)BNP. *Eur J Heart Fail*. 2004;6(3):257-260. [CrossRef]
5. Yamawaki H, Haendeler J, Berk BC. Thioredoxin: a key regulator of cardiovascular homeostasis. *Circ Res*. 2003;93(11):1029-1033. [CrossRef]
6. Domingues A, Jolibois J, Marquet de Rougé P, Nivet-Antoine V. The emerging role of TXNIP in ischemic and cardiovascular diseases; A novel marker and therapeutic target. *Int J Mol Sci*. 2021;22(4):1693. [CrossRef]
7. Xiong B, Jha V, Min JK, Cho J. Protein disulfide isomerase in cardiovascular disease. *Exp Mol Med*. 2020;52(3):390-399. [CrossRef]
8. Kodali VK, Thorpe C. Oxidative protein folding and the Quiescin-sulfhydryl oxidase family of flavoproteins. *Antioxid Redox Signal*. 2010;13(8):1217-1230. [CrossRef]
9. Alon A, Grossman I, Gat Y, et al. The dynamic disulphide relay of quiescin sulphydryl oxidase. *Nature*. 2012;488(7411):414-418. [CrossRef]
10. Jonmundsson T, Steindorsdottir AE, Austin TR, et al. A proteomic analysis of atrial fibrillation in a prospective longitudinal cohort (AGES-Reykjavik study). *Europace*. 2023;25(11):euad320. [CrossRef]
11. Koenen M, Becher T, Pagano G, et al. Ablation of Prdm16 and beige fat identity causes vascular remodeling and elevated blood pressure. *Science*. 2026;391(6782):306-313. [CrossRef]
12. Mebazaa A, Vanpoucke G, Thomas G, et al. Unbiased plasma proteomics for novel diagnostic biomarkers in cardiovascular disease: identification of quiescin Q6 as a candidate biomarker of acutely decompensated heart failure. *Eur Heart J*. 2012;33(18):2317-2324. [CrossRef]
13. Suhre K, McCarthy MI, Schwenk JM. Genetics meets proteomics: perspectives for large population-based studies. *Nat Rev Genet*. 2021;22(1):19-37. [CrossRef]
14. Swerdlow DI, Kuchenbaecker KB, Shah S, et al. Selecting instruments for Mendelian randomization in the wake of genome-wide association studies. *Int J Epidemiol*. 2016;45(5):1600-1616. [CrossRef]
15. Ferkingstad E, Sulem P, Atlason BA, et al. Large-scale integration of the plasma proteome with genetics and disease. *Nat Genet*. 2021;53(12):1712-1721. [CrossRef]
16. Sun BB, Chiou J, Traylor M, et al. Plasma proteomic associations with genetics and health in the UK Biobank. *Nature*. 2023;622(7982):329-338. [CrossRef]
17. Gallagher MD, Chen-Plotkin AS. The post-GWAS era: from association to function. *Am J Hum Genet*. 2018;102(5):717-730. [CrossRef]
18. Zhang X, Yu W, Li Y, Wang A, Cao H, Fu Y. Drug development advances in human genetics-based targets. *MedComm*. 2024;5(2):e481. [CrossRef]
19. Bao X, Liang Y, Chang H, et al. Targeting proprotein convertase subtilisin/kexin type 9 (PCSK9): from bench to bedside. *Signal Transduct Target Ther*. 2024;9(1):13. [CrossRef]
20. Luo F, Das A, Khetarpal SA, et al. ANGPTL3 inhibition, dyslipidemia, and cardiovascular diseases. *Trends Cardiovasc Med*. 2024;34(4):215-222. [CrossRef]
21. Sun BB, Maranville JC, Peters JE, et al. Genomic atlas of the human plasma proteome. *Nature*. 2018;558(7708):73-79. [CrossRef]
22. Kurki MI, Karjalainen J, Palta P, et al. FinnGen provides genetic insights from a well-phenotyped isolated population. *Nature*. 2023;613(7944):508-518. [CrossRef]
23. Lyon MS, Andrews SJ, Elsworth B, Gaunt TR, Hemani G, Marcora E. The variant call format provides efficient and robust storage of GWAS summary statistics. *Genome Biol*. 2021;22(1):32. [CrossRef]
24. Nielsen JB, Thorolfsdottir RB, Fritsche LG, et al. Biobank-driven genomic discovery yields new insight into atrial fibrillation biology. *Nat Genet*. 2018;50(9):1234-1239. [CrossRef]
25. Nikpay M, Goel A, Won HH, et al. A comprehensive 1,000 Genomes-based genome-wide association meta-analysis of coronary artery disease. *Nat Genet*. 2015;47(10):1121-1130. [CrossRef]
26. Shah S, Henry A, Roselli C, et al. Genome-wide association and Mendelian randomisation analysis provide insights into the pathogenesis of heart failure. *Nat Commun*. 2020;11(1):163. [CrossRef]
27. Malik R, Chauhan G, Traylor M, et al. Multiancestry genome-wide association study of 520,000 subjects identifies 32 loci associated with stroke and stroke subtypes. *Nat Genet*. 2018;50(4):524-537. [CrossRef]
28. Zhou W, Kanai M, Wu KHH, et al. Global Biobank Meta-analysis Initiative: powering genetic discovery across human disease. *Cell Genomics*. 2022;2(10):100192. [CrossRef]
29. Watanabe K, Taskesen E, van Bochoven A, Posthuma D. Functional mapping and annotation of genetic associations with FUMA. *Nat Commun*. 2017;8(1):1826. [CrossRef]
30. Zhu Z, Zhang F, Hu H, et al. Integration of summary data from GWAS and eQTL studies predicts complex trait gene targets. *Nat Genet*. 2016;48(5):481-487. [CrossRef]
31. Hinrichs AS, Karolchik D, Baertsch R, Barber GP, Bejerano G, Clawson H, Diekhans M, Furey TS, Harte RA, Hsu F, Hillman-Jackson J, Kuhn RM, Pedersen JS, Pohl A, Raney BJ, Rosenbloom KR, Siepel A, Smith KE, Sugnet CW, Sultan-Qurraie A, Thomas DJ, Trumbower H, Weber RJ, Weirauch M, Zweig AS, Haussler D, Kent WJ. The UCSC Genome Browser Database: update 2006. *Nucleic Acids Res*. 2006;34:D590-8. [CrossRef]
32. Larsson SC, Butterworth AS, Burgess S. Mendelian randomization for cardiovascular diseases: principles and applications. *Eur Heart J*. 2023;44(47):4913-4924. [CrossRef]
33. Bowden J, Del Greco M F, Minelli C, Davey Smith G, Sheehan N, Thompson J. A framework for the investigation of pleiotropy in two-sample summary data Mendelian randomization. *Stat Med*. 2017;36(11):1783-1802. [CrossRef]
34. Greco M FD, Minelli C, Sheehan NA, Thompson JR. Detecting pleiotropy in Mendelian randomisation studies with summary data and a continuous outcome. *Stat Med*. 2015;34(21):2926-2940. [CrossRef]
35. Bowden J, Davey Smith G, Burgess S. Mendelian randomization with invalid instruments: effect estimation and bias detection through Egger regression. *Int J Epidemiol*. 2015;44(2):512-525. [CrossRef]

36. Verbanck M, Chen CY, Neale B, Do R. Detection of widespread horizontal pleiotropy in causal relationships inferred from Mendelian randomization between complex traits and diseases. *Nat Genet*. 2018;50(5):693-698. [CrossRef]
37. Bowden J, Davey Smith G, Haycock PC, Burgess S. Consistent estimation in Mendelian randomization with some invalid instruments using a weighted median estimator. *Genet Epidemiol*. 2016;40(4):304-314. [CrossRef]
38. Võsa U, Claringbould A, Westra HJ, et al. Large-scale cis- and trans-eQTL analyses identify thousands of genetic loci and polygenic scores that regulate blood gene expression. *Nat Genet*. 2021;53(9):1300-1310. [CrossRef]
39. Wang X, Huang T, Jia J. Proteome-wide Mendelian randomization analysis identified potential drug targets for atrial fibrillation. *J Am Heart Assoc*. 2023;12(16):e029003. [CrossRef]
40. Wang K, Li M, Hakonarson H. ANNOVAR: functional annotation of genetic variants from high-throughput sequencing data. *Nucleic Acids Res*. 2010;38(16):e164. [CrossRef]
41. Amendola LM, Dorschner MO, Robertson PD, et al. Actionable exomic incidental findings in 6503 participants: challenges of variant classification. *Genome Res*. 2015;25(3):305-315. [CrossRef]
42. Kircher M, Witten DM, Jain P, O'Roak BJ, Cooper GM, Shendure J. A general framework for estimating the relative pathogenicity of human genetic variants. *Nat Genet*. 2014;46(3):310-315. [CrossRef]
43. Boyle AP, Hong EL, Hariharan M, et al. Annotation of functional variation in personal genomes using RegulomeDB. *Genome Res*. 2012;22(9):1790-1797. [CrossRef]
44. Buniello A, Suveges D, Cruz-Castillo C, et al. Open Targets Platform: facilitating therapeutic hypotheses building in drug discovery. *Nucleic Acids Res*. 2025;53(D1):D1467-D1475. [CrossRef]
45. Bertoni D, Tsenkov M, Magana P, Nair S, Pidruchna I, Querino Lima Afonso M, Midlik A, Paramval U, Lawal D, Tanweer A, Last M, Patel R, Laydon A, Lasecki D, Dietrich N, Tomlinson H, Žídek A, Green T, Kovalevskiy O, Lau A, Kandathil S, Bordin N, Sillitoe I, Mirdita M, Jones D, Orengo C, Steinegger M, Fleming JR, and Velankar S. AlphaFold Protein Structure Database 2025: a redesigned interface and updated structural coverage. *Nucleic Acids Res*. 2026;54:D358-d362.
46. Deng YT, You J, He Y, et al. Atlas of the plasma proteome in health and disease in 53,026 adults. *Cell*. 2025;188(1):253-271.e7. [CrossRef]
47. Caillard A, Sadoune M, Cescau A, et al. QSOX1, a novel actor of cardiac protection upon acute stress in mice. *J Mol Cell Cardiol*. 2018;119:75-86. [CrossRef]
48. Folkersen L, Gustafsson S, Wang Q, et al. Genomic and drug target evaluation of 90 cardiovascular proteins in 30,931 individuals. *Nat Metab*. 2020;2(10):1135-1148. [CrossRef]
49. Yuan S, Chen J, Ruan X, et al. Cross-population GWAS and proteomics improve risk prediction and reveal mechanisms in atrial fibrillation. *Nat Commun*. 2025;16(1):6426. [CrossRef]
50. Ning Z, Huang Y, Lu H, et al. Novel drug targets for atrial fibrillation identified through Mendelian randomization analysis of the blood proteome. *Cardiovasc Drugs Ther*. 2024;38(6):1215-1222. [CrossRef]
51. Li S, Schooling CM. A phenome-wide association study of ABO blood groups. *BMC Med*. 2020;18(1):334. [CrossRef]
52. Raje S, Thorpe C. Inter-domain redox communication in flavoenzymes of the quiescin/sulfhydryl oxidase family: role of a thioredoxin domain in disulfide bond formation. *Biochemistry*. 2003;42(15):4560-4568. [CrossRef]
53. Grossman I, Yuval Aviram H, Armony G, et al. Single-molecule spectroscopy exposes hidden states in an enzymatic electron relay. *Nat Commun*. 2015;6:8624. [CrossRef]
54. Ilani T, Alon A, Grossman I, et al. A secreted disulfide catalyst controls extracellular matrix composition and function. *Science*. 2013;341(6141):74-76. [CrossRef]
55. Goudis CA, Kallergis EM, Vardas PE. Extracellular matrix alterations in the atria: insights into the mechanisms and perpetuation of atrial fibrillation. *Europace*. 2012;14(5):623-630. [CrossRef]
56. Frangogiannis NG. The extracellular matrix in ischemic and nonischemic heart failure. *Circ Res*. 2019;125(1):117-146. [CrossRef]
57. Maharaj AV, Ishida M, Rybak A, et al. QSOX2 Deficiency-induced short stature, gastrointestinal dysmotility and immune dysfunction. *Nat Commun*. 2024;15(1):8420. [CrossRef]
58. Hong L, Jiang YF, Chen M, et al. Role of SH2B3 R262W gene polymorphism and risk of coronary heart disease: a PRISMA-compliant meta-analysis. *Med (Baltim)*. 2018;97(48):e13436. [CrossRef]
59. Murphy MB, Yang Z, Subati T, et al. LNK/SH2B3 loss of function increases susceptibility to murine and human atrial fibrillation. *Cardiovasc Res*. 2024;120(8):899-913. [CrossRef]
60. Zhu X, Fang J, Jiang DS, et al. Exacerbating pressure overload-induced cardiac hypertrophy: novel role of adaptor molecule Src homology 2-B3. *Hypertension*. 2015;66(3):571-581. [CrossRef]
61. CARDIoGRAMplusC4D Consortium, Deloukas P, Kanoni S, et al. Large-scale association analysis identifies new risk loci for coronary artery disease. *Nat Genet*. 2013;45(1):25-33. [CrossRef]
62. Dichgans M, Malik R, König IR, et al. Shared genetic susceptibility to ischemic stroke and coronary artery disease: a genome-wide analysis of common variants. *Stroke*. 2014;45(1):24-36. [CrossRef]
63. Lindström S, Wang L, Smith EN, et al. Genomic and transcriptomic association studies identify 16 novel susceptibility loci for venous thromboembolism. *Blood*. 2019;134(19):1645-1657. [CrossRef]
64. Devallière J, Charreau B. The adaptor Lnk (SH2B3): an emerging regulator in vascular cells and a link between immune and inflammatory signaling. *Biochem Pharmacol*. 2011;82(10):1391-1402. [CrossRef]
65. Flister MJ, Hoffman MJ, Lemke A, et al. SH2B3 is a genetic determinant of cardiac inflammation and fibrosis. *Circ Cardiovasc Genet*. 2015;8(2):294-304. [CrossRef]
66. Wang W, Tang Y, Wang Y, et al. LNK/SH2B3 loss of function promotes atherosclerosis and thrombosis. *Circ Res*. 2016;119(6):e91-e103. [CrossRef]
67. Dou H, Kotini A, Liu W, et al. Oxidized phospholipids promote NETosis and arterial thrombosis in LNK(SH2B3) deficiency. *Circulation*. 2021;144(24):1940-1954. [CrossRef]
68. Alexander MR, Hank S, Dale BL, et al. A single nucleotide polymorphism in SH2B3/LNK promotes hypertension development and renal damage. *Circ Res*. 2022;131(9):731-747. [CrossRef]
69. Allenspach EJ, Shubin NJ, Cerosaletti K, et al. The autoimmune risk R262W variant of the adaptor SH2B3 improves survival in sepsis. *J Immunol*. 2021;207(11):2710-2719. [CrossRef]
70. Finan C, Gaulton A, Kruger FA, et al. The druggable genome and support for target identification and validation in drug development. *Sci Transl Med*. 2017;9(383):eaag1166. [CrossRef]

Supplementary Table 1 SNPs used as IVs for circulating QSOX1 in the INTERVAL study

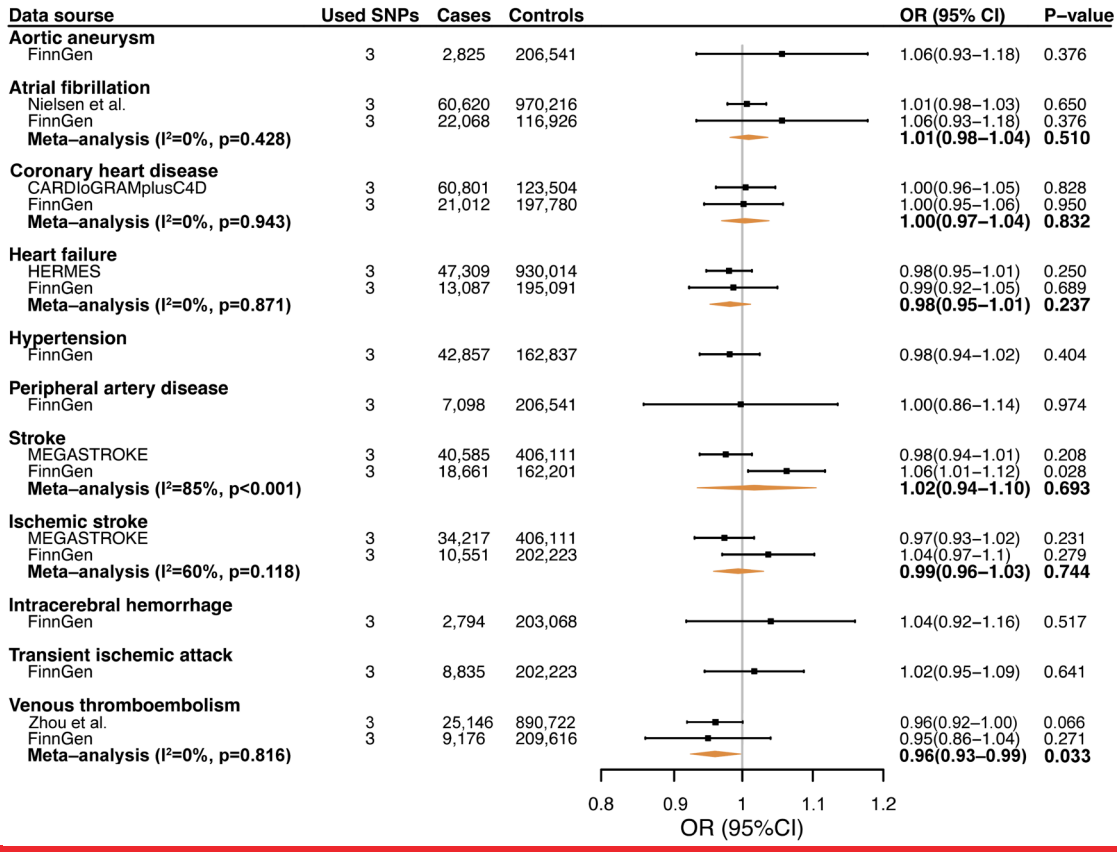
SNP	Chr	Position	EA	NEA	Beta	SE	*P*-value	F
rs12371	1	180163390	G	A	0.6995	0.0426	1.26E-60	284
rs12745791	1	180117914	G	A	-0.2717	0.0297	5.75E-20	86
rs357104	1	180182361	C	G	-0.1562	0.025	4.37E-10	41
rs79058837	1	180221629	T	C	0.1934	0.0352	4.07E-08	34

Chr, chromosome; EA, effect allele; NEA, non-effect allele; SE, standard error; SNP, single nucleotide polymorphisms.

Supplementary Table 2. SNPs used as IVs for circulating QSOX2 in the INTERVAL study

SNP	Chr	Position	EA	NEA	Beta	SE	*P*-value	F
rs550057	9	136146597	T	C	0.9028	0.024	1.00E-200	1428
rs10858248	9	139108324	G	A	-0.3568	0.0239	1.55E-50	224
rs28602660	9	136312071	A	G	0.6077	0.0433	8.32E-45	203
rs8176715	9	136133148	C	T	0.3394	0.0245	1.10E-43	199
rs3094373	9	136323826	T	A	-0.746	0.0578	4.79E-38	175
rs183853102	9	136219062	A	T	0.7301	0.0572	2.69E-37	174
rs78755596	9	136124590	A	T	0.825	0.0766	5.13E-27	133
rs7033492	9	136040986	C	T	0.2524	0.0269	6.61E-21	108
rs623179	9	136174678	T	C	0.2375	0.0263	1.62E-19	85
rs35434910	9	136042324	A	T	0.2481	0.0305	3.98E-16	70
rs652600	9	136311017	A	G	0.2134	0.0273	5.13E-15	65
rs76574146	9	139135964	G	T	-0.3297	0.0466	1.55E-12	58
rs9802874	9	136382716	G	A	-0.1918	0.0263	3.24E-13	56
rs149189328	9	136080512	C	A	0.5704	0.0869	5.13E-11	53
rs35698328	9	136129112	T	C	-0.3113	0.0469	3.09E-11	51
rs34214264	9	139164164	T	C	0.2046	0.0306	2.14E-11	49
rs2285488	9	136277854	A	G	-0.2221	0.0318	2.82E-12	48
rs116851371	9	136169725	C	A	1.043	0.1732	1.74E-09	48
rs6597609	9	136081466	T	C	0.1928	0.0301	1.41E-10	46
rs72775494	9	136251025	T	C	0.4438	0.0664	2.29E-11	46
rs8176744	9	136131350	T	G	-0.3509	0.0602	5.50E-09	39
rs74921353	9	136168396	T	C	-0.2535	0.0411	6.76E-10	39
rs113703846	9	139126195	T	G	0.3625	0.0651	2.51E-08	36
rs4962127	9	136178277	A	G	-0.3566	0.0596	2.24E-09	35
rs35565187	9	136037161	A	G	0.6342	0.1126	1.82E-08	33
rs55988407	9	136156064	A	G	-0.2934	0.0537	4.68E-08	32

Chr, chromosome; EA, effect allele; NEA, non-effect allele; SE, standard error; SNP, single nucleotide polymorphisms.



Supplementary Figure 1 . Screening of associations between genetically predicted circulating QSOX1 levels and CVD risk. MR estimates for the effect of circulating QSOX1 on various cardiovascular outcomes are shown, derived from INTERVAL pQTL data and FinnGen GWAS plus disease-specific consortia. Results are displayed as odds ratios (ORs) with 95% confidence intervals (CIs).

Supplementary Table 3. Sensitivity analyses of associations between genetically predicted circulating QSOX1 levels and CVD risk in the INTERVAL study

		Weighted Median		MR-Egger		Pleiotropy		Heterogeneity	
Outcome	**Study/consortium**	**OR (95% CI)**	**P-value**	**OR (95% CI)**	**P-value**	**Intercept**	**P-value**	**Q**	***P*-value**
Aortic aneurysm	FinnGen	1.07 (0.95–1.20)	0.272	1.16 (0.92–1.41)	0.439	-0.042	0.536	1	0.528
Atrial fibrillation	Nielsen et al.	1.01 (0.98–1.03)	0.679	1.01 (0.95–1.06)	0.851	-0.001	0.991	0	0.818
	FinnGen	1.07 (0.94–1.21)	0.303	1.16 (0.92–1.41)	0.439	-0.042	0.536	1	0.528
Coronary artery disease	CARDIoGRAMplusC4D	1.00 (0.95–1.04)	0.894	0.97 (0.88–1.06)	0.609	0.015	0.526	2	0.467
	FinnGen	1.00 (0.95–1.06)	0.891	1.01 (0.90–1.13)	0.870	-0.004	0.873	0	0.964
Heart failure	HERMES	0.99 (0.95–1.02)	0.439	1.02 (0.95–1.08)	0.716	-0.016	0.440	2	0.382
	FinnGen	0.99 (0.92–1.05)	0.682	0.98 (0.86–1.11)	0.835	0.002	0.951	0	0.982
Hypertension	FinnGen	0.99 (0.94–1.03)	0.593	1.01 (0.92–1.09)	0.919	-0.010	0.646	1	0.654
Peripheral artery disease	FinnGen	1.00 (0.91–1.10)	0.951	1.16 (0.97–1.35)	0.364	-0.066	0.320	6	0.051
Stroke	MEGASTROKE	0.97 (0.93–1.01)	0.168	0.96 (0.89–1.04)	0.513	0.006	0.755	0	0.814
	FinnGen	1.06 (1.01–1.12)	0.031	1.08 (0.97–1.19)	0.391	-0.008	0.765	0	0.928
Ischemic stroke	MEGASTROKE	0.97 (0.93–1.02)	0.251	0.95 (0.87–1.04)	0.473	0.010	0.669	0	0.848
	FinnGen	1.04 (0.97–1.11)	0.294	1.04 (0.91–1.17)	0.673	-0.001	0.980	0	0.998
Intracerebral hemorrhage	FinnGen	1.04 (0.90–1.17)	0.585	1.02 (0.77–1.26)	0.922	0.011	0.858	1	0.611
Transient ischemic attack	FinnGen	1.01 (0.93–1.09)	0.785	1.00 (0.85–1.14)	0.968	0.009	0.802	1	0.763
Venous thromboembolism	Zhou et al.	0.96 (0.92–1.00)	0.086	0.95 (0.86–1.05)	0.513	0.004	0.856	2	0.471
	FinnGen	0.94 (0.87–1.02)	0.137	0.90 (0.68–1.12)	0.526	0.024	0.677	3	0.188

CARDIoGRAMplusC4D, Coronary ARtery DIsease Genome wide Replication and Meta-analysis plus The Coronary Artery Disease Genetics; HERMES, Heart Failure Molecular Epidemiology for Therapeutic Targets.

Supplementary Table 4. Sensitivity analyses of associations between genetically predicted circulating QSOX2 levels and CVD risk in the INTERVAL study

		Weighted Median		MR-Egger		Pleiotropy		Heterogeneity	
Outcome	**Study/consortium**	**OR (95% CI)**	**P-value**	**OR (95% CI)**	**P-value**	**Intercept**	**P-value**	**Q**	***P*-value**
Aortic aneurysm	FinnGen	1.00 (0.94–1.06)	0.962	1.00 (0.93-1.09)	0.878	-0.005	0.782	16	0.897
Atrial fibrillation	Nielsen et al.	1.00 (0.97–1.02)	0.798	1.01 (0.95–1.08)	0.739	-0.005	0.664	24	<0.001
	FinnGen	1.06 (1.03–1.09)	<0.001	1.07 (1.01–1.13)	0.048	-0.008	0.534	49	0.002
Coronary artery disease	CARDIoGRAMplusC4D	1.07 (1.05–1.09)	<0.001	1.08 (1.04–1.12)	0.001	-0.004	0.632	36	0.030
	FinnGen	1.04 (1.01–1.06)	0.005	1.04 (1.00–1.08)	0.078	-0.001	0.914	27	0.284
Heart failure	HERMES	1.05 (1.04–1.07)	<0.001	1.05 (1.02–1.08)	0.005	-0.004	0.473	23	0.243
	FinnGen	1.04 (1.01–1.07)	0.011	1.05 (1.00–1.10)	0.073	-0.009	0.429	38	0.037
Hypertension	FinnGen	1.01 (0.99–1.03)	0.395	1.02 (0.99–1.06)	0.217	-0.009	0.232	34	0.090
Peripheral artery disease	FinnGen	1.02 (0.99–1.06)	0.214	1.03 (0.98–1.09)	0.248	-0.003	0.787	24	0.447
Stroke	MEGASTROKE	1.03 (1.00–1.05)	0.080	1.07 (1.01–1.13)	0.033	-0.014	0.151	27	0.084
	FinnGen	1.04 (1.02–1.07)	0.001	1.05 (1.01–1.09)	0.025	0.001	0.972	26	0.311
Ischemic stroke	MEGASTROKE	1.06 (1.03–1.10)	<0.001	1.08 (1.02–1.15)	0.022	-0.012	0.267	28	0.115
	FinnGen	1.04 (1.01–1.08)	0.005	1.05 (0.99–1.10)	0.155	0.001	0.924	40	0.014
Intracerebral hemorrhage	FinnGen	0.98 (0.92–1.03)	0.411	1.00 (0.92–1.08)	0.930	-0.005	0.763	19	0.701
Transient ischemic attack	FinnGen	1.02 (0.98–1.05)	0.373	1.02 (0.97–1.06)	0.476	0.003	0.797	15	0.909
Venous thromboembolism	Zhou et al.	1.21 (1.15–1.28)	<0.001	1.31 (0.98–1.74)	0.092	-0.025	0.618	15	<0.001
	FinnGen	1.18 (1.09–1.27)	<0.001	1.29 (1.05–1.54)	0.059	-0.029	0.496	108	<0.001

CARDIoGRAMplusC4D, Coronary ARtery DIsease Genome wide Replication and Meta-analysis plus The Coronary Artery Disease Genetics; HERMES, Heart Failure Molecular Epidemiology for Therapeutic Targets.

Supplementary Table 5. Associations of genetically predicted circulating QSOX1 and QSOX2 levels with CVD risk in the MR-PRESSO analysis

		QSOX1						QSOX2					
Outcome	Study/consortium	Used SNPs	Outliers	p_glo	p_dis	OR (95% CI)	P-value	Used SNPs	Outliers	p_glo	p_dis	OR (95% CI)	P-value
Aortic aneurysm	FinnGen	3	0	NA	NA	NA	NA	25	0	0.903	NA	NA	NA
Atrial fibrillation	Nielsen et al.	3	0	NA	NA	NA	NA	25	1	<0.001	0.187	1.01 (0.99–1.03)	0.382
	FinnGen	3	0	NA	NA	NA	NA	25	2	0.004	0.951	1.05 (1.03–1.07)	<0.001
Coronary artery disease	CARDIoGRAMplusC4D	3	0	NA	NA	NA	NA	23	0	0.049	NA	NA	NA
	FinnGen	3	0	NA	NA	NA	NA	25	0	0.334	NA	NA	NA
Heart failure	HERMES	3	0	NA	NA	NA	NA	20	0	0.150	NA	NA	NA
	FinnGen	3	0	NA	NA	NA	NA	25	1	0.045	0.760	1.04 (1.01–1.06)	0.007
Hypertension	FinnGen	3	0	NA	NA	NA	NA	25	0	0.126	NA	NA	NA
Peripheral artery disease	FinnGen	3	0	NA	NA	NA	NA	25	0	0.465	NA	NA	NA
Stroke	MEGASTROKE	3	0	NA	NA	NA	NA	19	0	0.074	NA	NA	NA
	FinnGen	3	0	NA	NA	NA	NA	24	0	0.384	NA	NA	NA
Ischemic stroke	MEGASTROKE	3	0	NA	NA	NA	NA	21	0	0.091	NA	NA	NA
	FinnGen	3	0	NA	NA	NA	NA	24	0	0.023	NA	NA	NA
Intracerebral hemorrhage	FinnGen	3	0	NA	NA	NA	NA	24	0	0.703	NA	NA	NA
Transient ischemic attack	FinnGen	3	0	NA	NA	NA	NA	24	0	0.921	NA	NA	NA
Venous thromboembolism	Zhou et al.	3	0	NA	NA	NA	NA	16	5	<0.001	1	1.25 (1.18–1.32)	0.002
	FinnGen	3	0	NA	NA	NA	NA	17	5	<0.001	0.749	1.20 (1.11–1.29)	0.002

CARDIoGRAMplusC4D, Coronary ARtery DIsease Genome wide Replication and Meta-analysis plus The Coronary Artery Disease Genetics; HERMES, Heart Failure Molecular Epidemiology for Therapeutic Targets.

Supplementary Table 6 Cis SNPs used as IVs for circulating QSOX2 in the deCODE study

SNP	Chr	Position	EA	NEA	Beta	SE	*P*-value	F
rs11103373	9	139085865	T	C	-0.2832	0.0087	1.48E-231	1055
rs76574146	9	139135964	G	T	-0.3797	0.0158	1.37E-127	577
rs34214264	9	139164164	T	C	0.2127	0.0107	4.36E-88	396
rs10117333	9	139099451	C	A	-0.2423	0.0179	1.45E-41	182
rs78498119	9	139143211	T	C	-0.344	0.0310	1.07E-28	124
rs73560761	9	139142668	T	C	0.1407	0.0127	1.43E-28	123
rs3125002	9	139405361	G	A	-0.0818	0.0088	1.16E-20	87
rs182762921	9	139102054	T	C	-0.2131	0.0229	1.34E-20	87
rs78378925	9	139059318	A	G	0.1636	0.0179	5.22E-20	84
rs11103249	9	138877437	A	G	-0.3016	0.0330	6.28E-20	84
rs77222745	9	139153608	A	G	-0.1315	0.0149	8.96E-19	78
rs959017	9	138998370	G	C	-0.082	0.0098	7.00E-17	70
rs75837171	9	139388636	G	C	0.1588	0.0191	8.73E-17	69
rs10870065	9	139352946	G	C	0.0725	0.0089	3.16E-16	67
rs72773794	9	139118515	T	C	-0.1821	0.0226	6.80E-16	65
rs113189561	9	139098942	A	G	0.2181	0.0292	8.62E-14	56
rs74893449	9	138970715	A	G	-0.1567	0.0217	5.69E-13	52
rs3812553	9	139256495	T	G	-0.1285	0.0183	2.18E-12	49
rs55683566	9	139109573	A	G	-0.2045	0.0291	2.21E-12	49
rs138639772	9	139080866	T	C	0.2692	0.0415	8.72E-11	42
rs140726899	9	138645310	A	G	-0.2011	0.0311	9.86E-11	42
rs79679719	9	139150685	G	A	-0.165	0.0264	3.93E-10	39
rs35667158	9	139157653	G	T	0.0808	0.0129	4.08E-10	39
rs11103200	9	138747408	C	A	-0.0906	0.0146	5.91E-10	38
rs34356735	9	139091521	A	G	0.1698	0.0276	7.75E-10	38
rs73557241	9	138673074	A	G	-0.1056	0.0173	1.14E-09	37
rs57837204	9	139064322	T	C	0.0845	0.0141	2.02E-09	36
rs185808769	9	139158141	G	C	0.135	0.0226	2.21E-09	36
rs11103246	9	138874793	C	T	0.0575	0.0098	4.67E-09	34
rs79374649	9	139025410	A	G	-0.1529	0.0264	7.27E-09	33
rs12550997	9	138772772	C	T	0.0553	0.0097	1.13E-08	33
rs144714013	9	139113341	G	C	0.1464	0.0257	1.15E-08	33
rs914738	9	139522005	C	T	0.053	0.0096	3.07E-08	31

Chr, chromosome; EA, effect allele; NEA, non-effect allele; SE, standard error; SNP, single nucleotide polymorphisms.